

# Refined Estimation of Kinetic Parameters of the Na<sup>+</sup>/H<sup>+</sup> Antiport in Human Fibroblasts and Platelets (43073)

JEFFREY P. GARDNER,<sup>1</sup> GORO TOKUDOME, HARUO TOMONARI, MORDECHAI ALADJEM,  
EDWARD CRAGOE, JR.,\* AND ABRAHAM AVIV

*Hypertension Research Center and Department of Physiology, University of Medicine and Dentistry of New Jersey,  
Newark, NJ 07103 and P.O. Box 631548,\* Nacogdoches, Texas 75963-1548*

---

**Abstract.** A technique is presented to estimate the initial rates of Na<sup>+</sup>-dependent alkalization of acidified human fibroblasts and platelets and assess the kinetics of the Na<sup>+</sup>/H<sup>+</sup> antiport in these cells. Cytosolic pH (pH<sub>i</sub>) exhibits an exponential recovery following cellular acidification. Thus, the length of the time interval selected to monitor changes in pH (ΔpH<sub>i</sub>) is critical to estimating the kinetics of the Na<sup>+</sup>/H<sup>+</sup> antiport. We compared kinetic parameters of the Na<sup>+</sup>/H<sup>+</sup> antiport, using computed and observed changes in ΔpH<sub>i</sub>, for arbitrarily selected time intervals following Na<sup>+</sup>-dependent activation. In both cells, significant increases in both the [Na<sup>+</sup>] for half-maximal activation (K<sub>0.5</sub>) and maximal velocities (V<sub>max</sub>) were observed as ΔpH<sub>i</sub> was decreased. We conclude that kinetic parameters derived from initial rate determinations enable a more accurate characterization of the Na<sup>+</sup>/H<sup>+</sup> antiport.

[P.S.E.B.M. 1990, Vol 194]

---

The Na<sup>+</sup>/H<sup>+</sup> antiport (exchange) has been the focus of numerous investigations during the last decade. Driven by the Na<sup>+</sup> and proton gradients across the plasma membrane, this transport system participates in a variety of biologic processes including the mitogenic response (1–3), stimulus-response coupling in white blood cells and platelets (4–6), vascular smooth muscle cell activation (7, 8), and Na<sup>+</sup> reabsorption by the renal proximal tubule (9). Indirect evidence also suggests that the Na<sup>+</sup>/H<sup>+</sup> antiport is involved in pathophysiologic conditions such as essential hypertension (10) and tumor growth (11).

The Na<sup>+</sup>/H<sup>+</sup> antiport is usually dormant at cytosolic pH (pH<sub>i</sub>) that is higher than pH 7.1–7.2 (4, 12). However, various agonists that stimulate the exchanger appear to exert their effect by shifting the pH<sub>i</sub> set point for its activation to a more alkaline pH (2, 13). Some of this effect may also be mediated by a rise in cytosolic free Ca<sup>2+</sup> (6, 8, 14, 15).

Amiloride and its 5-*N*-substituted analogues generally inhibit the Na<sup>+</sup>/H<sup>+</sup> antiport, and they have been extensively used as probes for this transport system (16). However, parameters of activation kinetics of the Na<sup>+</sup>/H<sup>+</sup> antiport have been obtained primarily by altering the pH<sub>i</sub> and Na<sup>+</sup> gradient across the plasma membrane. Two main approaches have been employed to determine these parameters. One is based on measurements of Na<sup>+</sup> transport and utilizes tracers such as <sup>22</sup>Na<sup>+</sup> (1, 12, 15–18). A second method relies on monitoring the pH<sub>i</sub> with intracellularly incorporated fluorescent dyes such as 2',7'-bis(carboxyethyl)-5,6-carboxyfluorescein (BCECF) (2, 4, 6–8). Both approaches usually resort to cellular acidification to activate the Na<sup>+</sup>/H<sup>+</sup> antiport and the subsequent measurement of the effect of altered transcellular Na<sup>+</sup> and proton gradients on the rates of <sup>22</sup>Na<sup>+</sup> transport (uptake or wash-out) and pH<sub>i</sub> recovery. A third, indirect approach for the measurement of the activity of the Na<sup>+</sup>/H<sup>+</sup> antiport has also been introduced. It measures cellular volume changes associated with activation of the exchanger by sodium propionate (4, 10, 19). Propionic acid rapidly moves into the cell causing cytosolic acidification, thereby activating the Na<sup>+</sup>/H<sup>+</sup> antiport, which, in turn, accelerates Na<sup>+</sup> uptake. The obligatory influx of water that occurs to maintain the cellular osmolality is measured by changes in cellular volume.

---

<sup>1</sup> To whom requests for reprints should be addressed at Department of Physiology, University of Medicine and Dentistry of New Jersey, 185 South Orange Avenue, Newark, NJ 07103.

---

Received July 14, 1989. [P.S.E.B.M. 1990, Vol 194]  
Accepted February 22, 1990.

---

0037-9727/90/1942-0165\$2.00/0  
Copyright © 1990 by the Society for Experimental Biology and Medicine

---

Irrespective of the method used, the accurate determination of parameters of the  $\text{Na}^+/\text{H}^+$  antiport depends on a reliable assessment of the rate of initial changes in  $\text{pH}_i$ ,  $\text{Na}^+$  transport, and cellular volume associated with activation of the exchanger. These changes are quite rapid, and techniques, as well as theoretical considerations used to obtain them, provide only rough estimations for parameters of activation kinetics of the exchanger. In this communication, we describe, (i) methodology to obtain a better characterization of the  $\text{Na}^+/\text{H}^+$  antiport, using monolayers of cultured human skin fibroblasts and suspensions of human platelets; and (ii) conclusions derived from the use of this methodology concerning the behavior of the antiport.

## Materials and Methods

**Cell Preparation.** Fibroblasts (passages 5–8) originated from skin biopsies of four normotensive subjects as previously described (18). They were grown in Dulbecco's modified Eagle's medium (95% air–5%  $\text{CO}_2$ ) with 10% fetal bovine serum, 2 mM L-glutamine, and antibiotics (50  $\mu\text{g}$  of streptomycin and 50 units of penicillin/ml). Four days prior to experiments,  $5 \times 10^5$  cells were inoculated into Nunc 6-well (35 mm in diameter) clusters. Each well contained a 13.8-  $\times$  30-mm glass coverslip. Cells were grown to confluency on the coverslips ( $0.7\text{--}1.0 \times 10^6$  cells/coverslip) using the same medium but without antibiotics. Fetal bovine serum was removed 24 hr before experiments in order to attain quiescence.

For platelets, 30 ml of venous blood were obtained from four medication-free normotensive subjects. Blood was collected into acid citrate dextrose (20/1:v/v) consisting of 14 mM sodium citrate, 11.8 mM citric acid, and 18 mM dextrose. Blood was centrifuged at 200g for 10 min at room temperature. The supernatant fraction containing platelet-rich plasma was centrifuged at 1000g for 10 min. Cells were rinsed three times with nominally bicarbonate-free buffer and pelleted by 1000g (10 min) centrifugation. The buffer consisted of (in mM) NaCl, 140; KCl, 5; glucose, 10; EGTA, 0.2; and Hepes, 10 (pH 7.40). EGTA was omitted from the third washing, which also included 0.1% fatty acid-free bovine serum albumin (BSA). Estimation of cell purity with a Coulter Counter indicated this procedure yielded platelets with less than 1% contamination of white blood cells. Platelets were studied within 4 hr of blood collection.

**BCECF Loading.** Fibroblasts were incubated for 60 min at 37°C in fetal bovine serum-free DMEM plus 5  $\mu\text{M}$  BCECF-acetoxyethylmethyl ester. Coverslips were washed twice with bicarbonate-free, Hepes-buffered solution (HBS) containing (in mM) NaCl, 140; KCl, 5;  $\text{MgCl}_2$ , 1;  $\text{CaCl}_2$ , 2; glucose, 10; Hepes, 10 (pH 7.40); and 0.1% BSA. Platelets were loaded with 5  $\mu\text{M}$

BCECF-AM for 60 min at 37°C in HBS (without BSA) and 1 mM  $\text{CaCl}_2$ , instead of 2 mM  $\text{CaCl}_2$  used for fibroblasts.

**Cellular Acidification and Activation of the  $\text{Na}^+/\text{H}^+$  Antiport.** In studies by others, the nigericin-induced cellular acidification has often been performed using  $\text{K}^+$  concentrations that approximate the intracellular levels of the ion (12, 20). In our experiments, the  $\text{K}^+$  concentration in the acidifying buffer was maintained at 5 mM. Acidification at physiologic  $\text{K}^+$  concentration prevents activation of voltage-gated  $\text{Ca}^{2+}$  channels, which could take place when cells are depolarized by a high extracellular  $\text{K}^+$  concentration (14, 21, 22). The approach we adopted prevents a rise in cytosolic  $\text{Ca}^{2+}$  ( $[\text{Ca}^{2+}]_i$ ), which may alter the activity of the  $\text{Na}^+/\text{H}^+$  antiport in some cells (6, 8, 15).

Fibroblast acidification was carried out at 37°C for 5 min in HBS without BSA plus 0.5  $\mu\text{g}/\text{ml}$  nigericin (pH 6.60). Coverslips were secured at a 45° angle in the groove of a Teflon support block inserted at the bottom of a quartz cuvette. All solution changes were accomplished by removing media via a suction tube embedded in the block and then decanting freshly mixed solution along the sides of the cuvette. Cells were washed twice with  $\text{Na}^+$ -free HBS (pH 6.60,  $\text{Na}^+$  being replaced by *N*-methyl-D-glucamine) to remove nigericin. The antiport was activated by the addition of 3 ml of HBS of different  $\text{Na}^+$  concentrations (0–140 mM; maintained at 37°C, pH 7.40).

Platelets were acidified at room temperature in  $\text{Na}^+$ -free HBS (without BSA) containing 0.5  $\mu\text{g}/\text{ml}$  nigericin (pH 6.80). After 7-min exposure to acidification buffer, BSA was added (0.1%) to scavenge the nigericin (4). The  $\text{Na}^+/\text{H}^+$  exchanger was activated by adding 150- $\mu\text{l}$  aliquots (approximately  $3 \times 10^6$  platelets) to 3 ml of HBS (0.1% BSA) of different  $\text{Na}^+$  concentrations, as per fibroblasts. The 20-fold dilution of the nigericin plus 0.1% BSA eliminated any further effect of the ionophore.

The sensitivity of the  $\text{pH}_i$  recovery from acidification to the amiloride analogue 5-(*N*-methyl-*N*-isobutyl)amiloride (MIBA) was tested by exposure of the cells to HBS in the presence of different concentrations of the analogue. MIBA was synthesized by a previously described method (23). To calibrate  $\text{pH}_i$ , cells were subjected to HBS (minus BSA) of different pH values (6.40–7.50) with 5  $\mu\text{g}/\text{ml}$  nigericin and 145 mM  $\text{K}^+$  (isosmotically substituted for  $\text{Na}^+$ ) (8, 24). Standard curves were constructed for each preparation studied.

**pH<sub>i</sub> Monitoring.** Changes in  $\text{pH}_i$  were monitored under constant stirring at 37°C in a SPEX fluorolog II spectrofluorimeter (model CM-3). Excitation and emission wavelengths were set at 440/503 nm and 530 nm, respectively. The integration time was set at 0.2 sec and data points were obtained at 1-sec intervals. Autofluorescence of similarly prepared aliquots of platelets or

monolayers not exposed to BCECF-AM was measured for each experiment. Basal  $\text{pH}_i$  values for fibroblasts and platelets were  $6.93 \pm 0.14$  and  $7.27 \pm 0.05$  (mean  $\pm$  SD,  $n = 4$ ), respectively.

At the start of  $\text{Na}^+$  activation experiments, an artifactual decrease in  $\text{pH}_i$  was recorded due to room light flooding the cuvette chamber. We determined the elapsed time from addition of the  $\text{Na}^+/\text{H}^+$  antiport activating solution to the first data point (initial point, IP). These intervals were  $4.0 \pm 0.6$  sec (mean  $\pm$  SD) for fibroblasts ( $n = 8$ ) and  $2.1 \pm 0.4$  sec for platelets ( $n = 8$ ). Accordingly, IP was set at 4 sec (for fibroblasts) or 2 sec (for platelets) in subsequent curve fitting procedures.

**Data Analysis.** Fluorescent signals were corrected for autofluorescence and the 503:440 ratio converted to  $\text{pH}_i$  values. Three approaches were undertaken to estimate the rate of change in  $\text{pH}_i$  following activation of the  $\text{Na}^+/\text{H}^+$  antiport. The first approach was to measure the observed  $\text{pH}_i$  at two arbitrary time intervals of the  $\text{pH}_i$  recovery (10 and 30 sec after the IP for fibroblasts; 5 and 10 sec after IP for platelets). The other two approaches used computed rate constants of the exponential  $\text{pH}_i$  recovery curves, obtained through iterative curve fitting, as previously described (5, 11). For this analysis, data files were transferred to ASCII files using SPEX software. SAS PROCNLIN (25) was used to fit the data and estimate parameters of the curves (any program supporting user-defined equations for curve-fitting procedures would suffice). The following equation was used:

$$\text{pH}_{(t)} = \text{pH}_{(\infty)} - (\text{pH}_{(\infty)} - \text{pH}_{i,0})e^{-kt} \quad [1]$$

where  $\text{pH}_{(t)} = \text{pH}_i$  at a given time  $t$ ,  $\text{pH}_{(\infty)} =$  the  $\text{pH}_i$  at the new steady state,  $\text{pH}_{i,0} =$  the initial  $\text{pH}_i$  at the moment of activation of the  $\text{Na}^+/\text{H}^+$  antiport, and  $k =$  rate constant. Since the IP values were respectively obtained at 4 or 2 sec after activation of the  $\text{Na}^+/\text{H}^+$  antiport in fibroblasts and platelets, the  $\text{pH}_{i,0}$  was extrapolated from the fitted data (Fig. 1). The extrapolation of the curve to  $\text{pH}_{i,0}$  is based on the assumption that the pattern describing the  $\text{pH}_i$  increment from the IP to the new steady state ( $\text{pH}_{(\infty)}$ ) is representative of the  $\text{pH}_i$  profile from  $\text{pH}_{i,0}$  to the IP. For fibroblasts, the time interval between  $\text{pH}_{i,0}$  and IP was 3.5% and for platelets it was 10% of the entire  $\text{pH}_i$  monitoring period after activation of the  $\text{Na}^+/\text{H}^+$  antiport. Rate constants obtained from exponential curves were utilized to calculate (i) the initial rate of  $\text{pH}_i$  recovery described by the expression  $k(\text{pH}_{(\infty)} - \text{pH}_{i,0})$ , and (ii) the change in  $\text{pH}_i$  ( $\Delta\text{pH}_i$ ) at arbitrarily chosen time intervals from  $\text{pH}_{i,0}$  (1, 5, 10, and 30 sec for fibroblasts and 1, 5, and 10 sec for platelets).

Initial rates and observed or computed rates for  $\text{pH}_i$  were used to obtain the  $\text{Na}^+$  activation kinetic

parameters of the  $\text{Na}^+/\text{H}^+$  antiport according to the following model:

$$V = V_{\max} [\text{Na}^+]_o^n / K_{0.5}^n + [\text{Na}^+]_o^n \quad [2]$$

where  $v =$  change in  $\text{pH}_i$ ,  $V_{\max} =$  maximal velocity,  $[\text{Na}^+]_o =$  extracellular  $\text{Na}^+$  concentration,  $K_{0.5} = [\text{Na}^+]_o$  for half-maximal activation, and  $n =$  the Hill coefficient. Equation 2 is a modification of the Michaelis-Menten equation that introduces an index of cooperativity ( $n$ ). Estimation of kinetic parameters were obtained by curve fitting techniques using SAS PROCNLIN (25).

**Statistical Analysis.** Data are presented as mean or mean  $\pm$  SD. Statistical analysis was performed using Student's  $t$  test or one-way analysis of variance.

## Results

Illustrations of  $\text{Na}^+$ -dependent  $\text{pH}_i$  recovery for fibroblasts and platelets are shown in Figure 1. This figure demonstrates the relationship between the observed data and predicted  $\text{pH}_i$  change according to the model described by Equation 1. In general, there is an excellent fit of the model to data obtained during  $\text{Na}^+$  activation of both fibroblasts and platelets. In fibroblasts, experimentally determined  $\text{pH}_i$  values occasionally showed mild fluctuations about the exponential curve (e.g., Fig. 1A). The observed  $\text{pH}_i$  values for platelets fell on the computed exponential  $\text{pH}_i$  recovery curve.

The rate of  $\text{pH}_i$  recovery is substantially lower in fibroblasts than platelets. The  $\text{pH}_{i,0}$  values extrapolated from such curves were  $6.50 \pm 0.05$  for fibroblasts ( $n = 28$ ) and  $6.61 \pm 0.08$  for platelets ( $n = 28$ ). Thus, the lower rate of  $\text{pH}_i$  recovery in fibroblasts cannot be attributed to a higher  $\text{pH}_{i,0}$ .

$\text{Na}^+$ -dependent  $\text{pH}_i$  recovery is sensitive to MIBA in both fibroblasts and platelets (Fig. 2). The  $\text{pH}_i$  recovery of both cells is almost completely inhibited by the highest concentration of amiloride analogue tested, i.e.,  $10^{-5}$  M. Studies with other 5-( $N$ -substituted) amiloride analogues produced similar results (data not shown). Acidified fibroblasts and platelets exposed to  $\text{Na}^+$ -free HBS (pH 7.40) demonstrated little or no change in  $\text{pH}_i$  from initial values. These observations suggest that, under these experimental conditions, the  $\text{Na}^+$ -induced  $\text{pH}_i$  recovery in these cells is solely dependent on the  $\text{Na}^+/\text{H}^+$  antiport.

Figures 3 and 4 illustrate the kinetics of  $\text{Na}^+$ -dependent  $\text{pH}_i$  recovery for fibroblasts and platelets, respectively. Curves were constructed according to the model described by Equation 2, using initial rates and computed rates based on time intervals following  $\text{pH}_{i,0}$  (A) and observed rates using time intervals following IP (B). The use of initial rates results in the largest rate of change in  $\text{pH}_i$  units/sec (Figs. 3A and 4A). It is apparent that, irrespective of the approach used, the

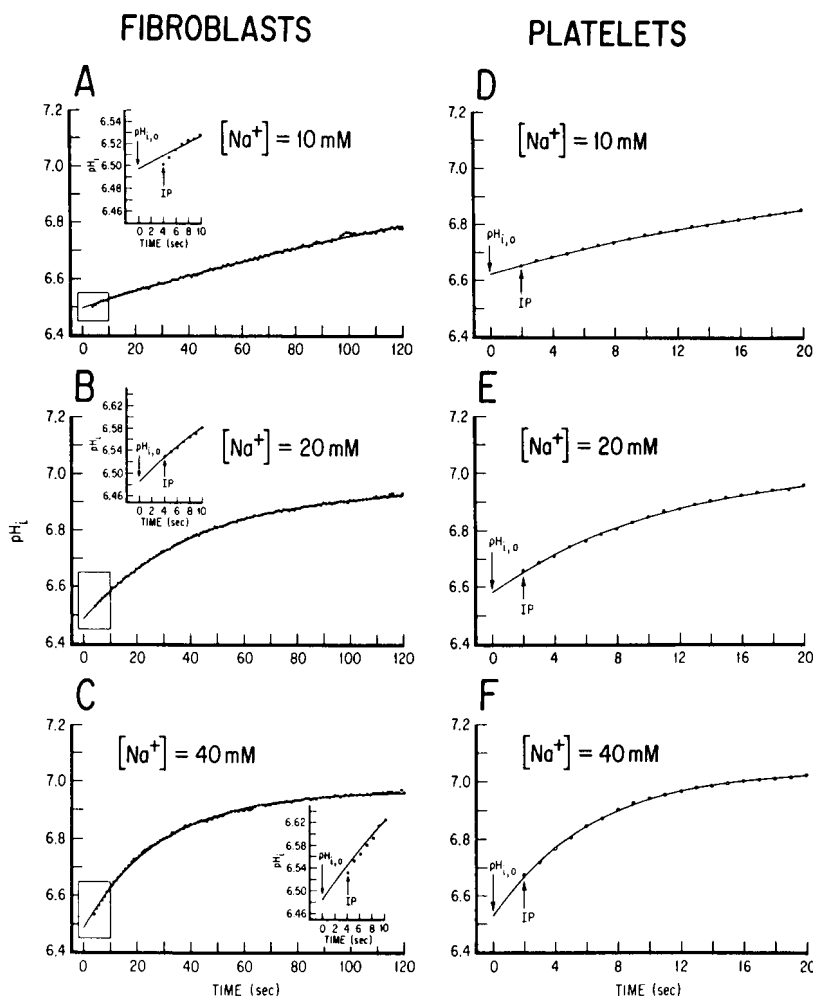


**Figure 1.**  $pH_i$  recovery of acidified fibroblasts (A–C) and platelets (D–F) as a function of  $[Na^+]_o$ . Cells were acidified as described in Materials and Methods, and  $pH_i$  measurements were recorded once cells were exposed to  $Na^+$ -containing solutions. Curves were fit to Equation 1 and both observed data and calculated curves were plotted with a software package (Graph Pad II). The rate constant ( $k$ ) values for these curves were (in  $sec^{-1}$ ): A, 0.0041; B, 0.0237; C, 0.0347; D, 0.0451; E, 0.0912; and F, 0.1582. Insets: the first 10 sec of  $pH_i$  recovery for fibroblasts are magnified to show initial  $pH_i$  measurements and calculated  $pH_i$  values.

longer the time interval following activation of the  $Na^+/H^+$  antiport, the lower the computed  $V_{max}$  value for the  $pH_i$  recovery. Kinetic parameters obtained from rates of  $pH_i$  changes confirm this impression for both fibroblasts (Table I) and platelets (Table II). These results indicate that not only the  $V_{max}$ , but also the  $K_{0.5}$  values progressively decline when longer time intervals are selected for measurements of  $pH_i$  changes following either the IP or  $pH_{i,0}$ .

Precise characterization of the  $Na^+/H^+$  antiport requires the determination of  $H^+$  equivalent efflux rates (product of the cell's buffer capacity and  $Na^+$ -dependent  $pH_i$  recovery). Since the buffer capacity for both human platelets and fibroblasts is approximately 20  $mmol\ liter^{-1}\ pH^{-1}$  (unpublished data), the maximum  $H^+$  equivalent efflux rates are approximately three times as high in platelets than in fibroblasts.

In fibroblasts, but not platelets, the Hill coefficient is significantly increased by the length of time following

IP or  $pH_{i,0}$ . Of interest is the observation that  $n$  values derived from initial rates and  $pH_i$  changes over short intervals are greater than unity in both cells. These results suggest positive cooperativity in  $Na^+$ -dependent  $pH_i$  recovery. Similar findings regarding the Hill coefficient have recently been reported in erythrocytes (26) and renal tubular epithelium (27).

## Discussion

Continuous monitoring of the rate of alkalinization following a cellular acid load provides an accurate and reliable assessment for the activation kinetics of the  $Na^+/H^+$  antiport. Methods that rely on measurements of changes in  $Na^+$  transport or cellular volume have several shortcomings that limit their accuracy.  $^{22}Na^+$  uptake experiments entail isolation of the cells from the bathing medium and their repeated washing to remove the extracellular tracer. These steps require a finite time and the initial and most important phase of

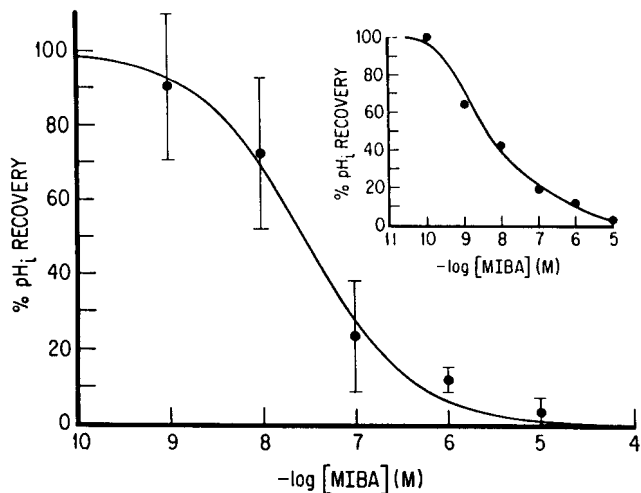


**Figure 2.** Dose-response curves for MIBA inhibition of  $\text{Na}^+$ -dependent  $\text{pH}_i$  recovery in fibroblasts ( $n = 3$ ) and platelets (inset, representative of one experiment). Fibroblasts and platelets were acidified as described in Materials and Methods and exposed to HBS containing  $140 \text{ mM Na}^+$  ( $\text{pH } 7.40$ ). Changes in  $\text{pH}_i$  for 10-sec intervals of MIBA-treated cells are expressed as a percentage of the average  $\Delta\text{pH}_i$  of three experiments performed in the absence of MIBA.

the uptake cannot be measured accurately (28). By following the appearance of  $^{22}\text{Na}^+$  in the extracellular compartment, it is possible to perform  $^{22}\text{Na}^+$  washout experiments in some cells without the necessity for their isolation from the bathing medium. Such a method could be further refined to estimate the initial rate of the washout (28). When the washout is performed under a steady-state condition with respect to cellular  $\text{Na}^+$ , the rate of  $^{22}\text{Na}^+$  uptake equals  $^{22}\text{Na}^+$  washout. Thus, the amiloride-sensitive component of the washout can be considered to represent the  $\text{Na}^+/\text{H}^+$  antiport. We have used this approach in previous investigations (17, 18). However, it cannot be applied to cell suspensions and for rapid measurements of activation kinetics of the antiport.

Monitoring changes in cellular volume following a  $\text{Na}^+$  propionate load (the cell sizing technique) may not

necessarily reflect the activity of the  $\text{Na}^+/\text{H}^+$  antiport. Changes in cellular volume are related not only to the activity of the  $\text{Na}^+/\text{H}^+$  antiport, but to other factors such as the  $\text{Na}^+-\text{K}^+$  ATPase ( $\text{Na}^+$ -pump). For instance, cells with a lower density of  $\text{Na}^+$ -pumps may demonstrate greater changes in volume associated with  $\text{Na}^+$  propionate loading irrespective of the activity of the  $\text{Na}^+/\text{H}^+$  antiport. Compared with cells with a higher number of  $\text{Na}^+$ -pumps, these cells are likely to reach a new steady state for  $\text{Na}^+$  extrusion at a slower pace or at  $\text{Na}^+$  concentrations that require a greater obligatory uptake of water.

Several aspects of our methodology and analyses of the results merit special considerations. Acidification of the cells, using relatively low concentrations of nigericin and  $\text{K}^+$ , prevents membrane depolarization and activation of voltage-gated  $\text{Ca}^{2+}$  channels. These channels are quite common in a variety of cells, and recently we (Hatori and Aviv, unpublished data) and others have demonstrated their existence in fibroblasts (14) and platelets (22). A rise in  $[\text{Ca}^{2+}]_i$  may alter the basal activity of the  $\text{Na}^+/\text{H}^+$  antiport, inasmuch as alterations in  $[\text{Ca}^{2+}]_i$  may modulate the activity of the exchanger (6, 8, 15). Our investigations show that in platelets, a rise in  $[\text{Ca}^{2+}]_i$  increases the activity of the  $\text{Na}^+/\text{H}^+$  antiport, whereas in cultured skin fibroblasts  $[\text{Ca}^{2+}]_i$  has no effect on the antiporter (Gardner, Kimura, and Aviv, unpublished data). A second feature of this methodology is that nigericin acidification at extracellular  $\text{K}^+$  concentrations lower than intracellular  $\text{K}^+$  levels results in lack of a priori knowledge regarding the  $\text{pH}_{i,o}$  of the acidified cells. However, this parameter is obtained by extrapolation from the  $\text{pH}_i$  recovery curve. The same approach can be adapted to alternative acidification methods such as sodium propionate addition and the  $\text{NH}_4\text{Cl}$  prepulse.

The activity of the  $\text{Na}^+/\text{H}^+$  antiport decelerates as the  $\text{pH}_i$  gradient across the plasma membrane declines and the  $\Delta\text{pH}_i$  following activation of the antiport cannot be linear at any phase of the  $\text{pH}_i$  increment. Thus,

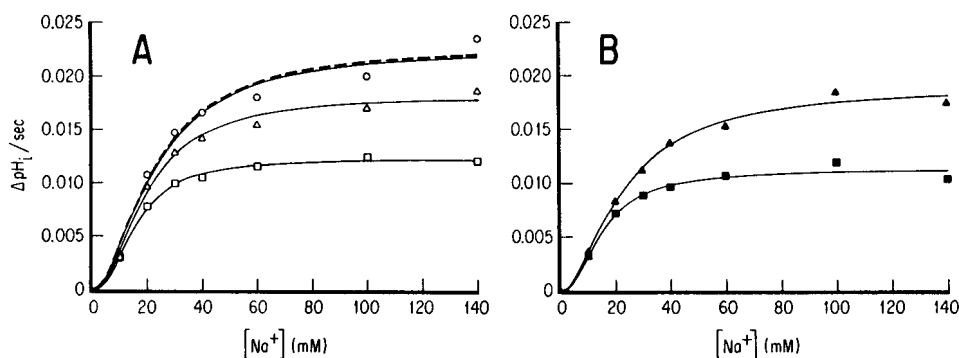


**Figure 3.** Initial velocities of  $\text{pH}_i$  recovery in fibroblasts as a function of  $[\text{Na}^+]_o$ . The initial rates and changes in  $\text{pH}_i$ , obtained from experiments similar to those depicted in Figure 1 at  $[\text{Na}^+]_o$  of  $10\text{--}140 \text{ mM}$ , were calculated and used to estimate kinetic parameters according to Equation 2. Curves were plotted using Graph Pad II. Initial rate (---) and calculated  $\Delta\text{pH}_i$  of 1 sec ( $\circ$ ), 5 sec ( $\Delta$ ), and 30 sec ( $\square$ ) are shown in A. Observed  $\Delta\text{pH}_i$  of 10 sec ( $\blacktriangle$ ) and 30 sec ( $\blacksquare$ ) are shown in B.

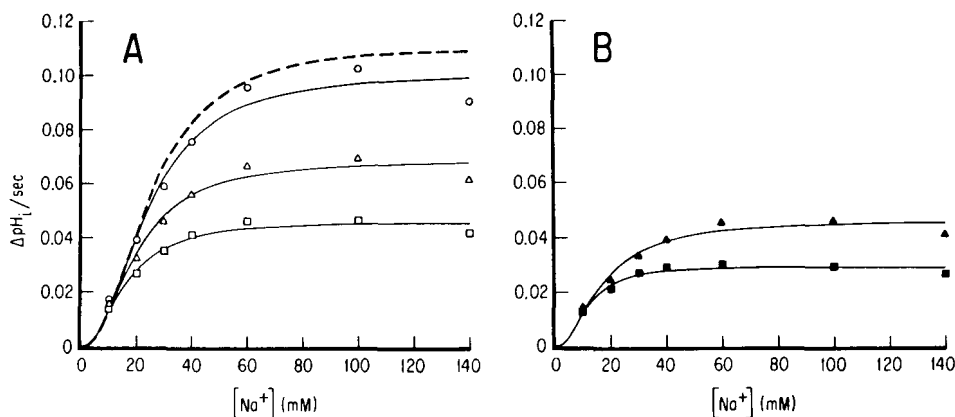


**Figure 4.** Initial velocities of  $\Delta pH_i$  recovery in platelets as a function of  $[Na^+]_o$ . Initial rate (---) and calculated  $\Delta pH_i$  of 1 sec (○), 5 sec (Δ), and 10 sec (□) for A, and observed  $\Delta pH_i$  of 5 sec (▲) and 10 sec (■) for B are as per legend to Figure 3.

**Table I.** Kinetic Parameters of  $Na^+$ -Dependent Activation of  $Na^+$ - $H^+$  Exchange in Cultured Skin Fibroblasts<sup>a</sup>

Parameter	$k(pH_{i(\infty)} - pH_{i,o})$	Calculated (from Equation 1) time following $pH_{i,o}$ (sec)				$p^b$	Observed time following IP (sec)		$p^c$
		1	5	10	30		10	30	
$V_{max}$ (pH <sub>i</sub> /sec)	0.037 ±0.009	0.032 ±0.008	0.029 ±0.007	0.025 ±0.005	0.015 ±0.003	0.007	0.023 ±0.004	0.012 ±0.002	0.003
$K_{0.5}$ (mM $Na^+$ )	21.7 ±1.3	21.6 ±3.8	20.3 ±2.0	18.3 ±1.9	13.8 ±1.9	0.001	20.7 ±1.8	11.8 ±2.4	0.001
$n$	1.6 ±0.2	1.9 ±0.2	1.8 ±0.4	1.9 ±0.2	2.2 ±0.5	0.054	1.6 ±0.2	2.2 ±0.4	0.025

<sup>a</sup> Values represent mean ± SD of four separate experiments.

<sup>b</sup> Calculated by analysis of variance.

<sup>c</sup> Calculated by Student's *t* test.

**Table II.** Kinetic Parameters of  $Na^+$ -Dependent Activation of  $Na^+$ - $H^+$  Exchange in Platelets<sup>a</sup>

Parameter	$k(pH_{i(\infty)} - pH_{i,o})$	Calculated (from Equation 1) time following $pH_{i,o}$ (sec)			$p^b$	Observed time following IP (sec)		$p^c$
		1	5	10		5	10	
$V_{max}$ (pH <sub>i</sub> /sec)	0.125 ±0.029	0.113 ±0.022	0.072 ±0.007	±0.004	0.048 <0.001	0.048 ±0.005	0.029 ±0.004	<0.001
$K_{0.5}$ (mM $Na^+$ )	33.5 ±5.8	33.1 ±6.4	25.2 ±3.7	20.8 ±3.4	0.009	21.7 ±4.6	14.8 ±3.0	0.047
$n$	1.9 ±0.3	1.9 ±0.4	1.9 ±0.3	1.9 ±0.4	0.983	1.8 ±0.5	2.0 ±0.4	0.513

<sup>a</sup> Values represent mean ± SD of four separate experiments.

<sup>b</sup> Calculated by analysis of variance.

<sup>c</sup> Calculated by Student's *t* test.

rates of  $pH_i$  changes that are derived from increasingly longer time intervals following activation of the  $Na^+$ / $H^+$  antiport yield less reliability in measurements of activation kinetics of the exchanger. This conclusion holds even when an increase in  $pH_i$  appears to fall within the linear phase of the  $pH_i$  recovery. Iterative curve fittings of the entire  $pH_i$  profile after activation of the  $Na^+$ / $H^+$  antiport and extrapolation to  $pH_{i,o}$  pro-

vide greater precision in calculating the exponential parameters of the  $Na^+$ -dependent  $pH_i$  recovery. Hence, kinetic parameters obtained using initial rate determinations describe the  $Na^+$ / $H^+$  antiport with a better accuracy since they represent the instantaneous velocity of the transport system. This concept may not be of a great importance when experiments are designed to test the presence or absence of the antiport in a given cell

and its contribution to a physiologic or biologic process. However, it becomes essential, when a quantitative evaluation of parameters of the  $\text{Na}^+/\text{H}^+$  antiport is necessary to explain physiologic or pathophysiologic processes that may be linked to the behavior of this transport system.

This work was supported by Grant HL34807 from the National Heart Lung and Blood Institute and a grant-in-aid from the American Heart Association, NJ affiliate.

We thank Marietta Mascarina and Amy Michaelsky for their technical skills and Norma Hernandez for her secretarial expertise.

1. Moolenaar WH, Mummery CL, Van der Saag PT, de Laat SW. Rapid ionic events and the initiation of growth in serum stimulated neuroblastoma cells. *Cell* **23**:789-798, 1981.
2. Moolenaar WH, Tsein RY, Van der Saag PT, de Laat SW.  $\text{Na}^+/\text{H}^+$  exchange and cytoplasmic pH in the action of growth factors in human fibroblasts. *Nature* **304**:645-648, 1983.
3. Pouyssegur J, Chambard JC, Franchi A, Paris S, Van Obberghen-Schilling E. Growth factor activation of an amiloride-sensitive  $\text{Na}^+/\text{H}^+$  exchange system in quiescent fibroblasts: Coupling to ribosomal S6 phosphorylation. *Proc Natl Acad Sci USA* **79**:3935-3939, 1982.
4. Grinstein S, Furuya W. Characterization of the amiloride-sensitive  $\text{Na}^+/\text{H}^+$  antiport of human neutrophils. *Am J Physiol* **250**:C283-C291, 1986.
5. Simchowicz L. Intracellular pH modulates the generation of superoxide radicals by human neutrophils. *J Clin Invest* **76**:1079-1089, 1985.
6. Zavoico GB, Cragoe EJ Jr, Feinstein MB. Regulation of intracellular pH in human platelets. *J Biol Chem* **261**:13160-13167, 1986.
7. Berk BC, Aronow MS, Brock TA, Cragoe E, Gimbrone MA, Alexander RW. Angiotensin II-stimulated  $\text{Na}^+/\text{H}^+$  exchange in cultured vascular smooth muscle cells. Evidence for protein kinase C-dependent and -independent pathways. *J Biol Chem* **262**:5057-5064, 1987.
8. Hatori N, Fine BP, Nakamura A, Cragoe E, Aviv A. Angiotensin II effect on cytosolic pH in cultured rat vascular smooth muscle cells. *J Biol Chem* **262**:5073-5078, 1987.
9. Boron WF, Boulpaep EL. Intracellular pH regulation in the renal proximal tubule of the salamander. Na-H exchange. *J Gen Physiol* **81**:29-52, 1983.
10. Livne A, Balfe JW, Veitch R, Marquez-Julio A, Grinstein S, Rothstein A. Increased platelet  $\text{Na}^+/\text{H}^+$  exchange rates in essential hypertension: application of a novel test. *Lancet* **1**:533-536, 1987.
11. Bierman AJ, Tertoolen LGJ, de Laat SW, Moolenaar WH. The  $\text{Na}^+/\text{H}^+$  exchanger is constitutively activated in P19 embryonal carcinoma cells, but not in a differentiated derivative. *J Biol Chem* **262**:9621-9628, 1987.
12. Vigne P, Frelin C, Lazdunski M. The  $\text{Na}^+$  dependent regulation of the internal pH in chick skeletal muscle cells. The role of the  $\text{Na}^+/\text{H}^+$  exchange system and its dependence on internal pH. *EMBO J* **3**:1865-1870, 1984.
13. Aronson PS, Nee J, Suhn MA. Modifier role of internal  $\text{H}^+$  in activating the  $\text{Na}^+/\text{H}^+$  exchanger in renal microvillus membrane vesicles. *Nature* **299**:161-163, 1982.
14. Chen C, Corbley MJ, Roberts TM, Hess P. Voltage-sensitive calcium channels in normal and transformed 3T3 fibroblasts. *Science* **239**:1024-1026, 1988.
15. Owen NE, Villereal ML. Evidence for a role of calmodulin in serum stimulation of  $\text{Na}^+$  influx in human fibroblasts. *Proc Natl Acad Sci USA* **79**: 3537-3541, 1982.
16. Vigne P, Frelin C, Cragoe EJ, Lazdunski M. Structure activity relationships of amiloride and certain of its analogues in relation to the blockade of the  $\text{Na}^+/\text{H}^+$  exchange system. *Mol Pharmacol* **25**:131-136, 1984.
17. Kuriyama S, Denny T, Aviv A.  $^{22}\text{Na}^+$  and  $^{86}\text{Rb}^+$  transport in vascular smooth muscle of SHR, Wistar Kyoto and Wistar rats. *J Cardiovasc Pharmacol* **11**:722-729, 1988.
18. Kuriyama S, Hopp L, Tamura H, Lasker N, Aviv A. A higher cellular sodium turnover rate in cultured skin fibroblasts from blacks. *Hypertension* **11**:301-307, 1988.
19. Grinstein S, Goetz JD, Furuya W, Rothstein A, Gelfand EW. Amiloride-sensitive  $\text{Na}^+/\text{H}^+$  exchange in platelets and leukocytes: Detection by electronic cell sizing. *Am J Physiol* **247**:C293-C298, 1984.
20. Grinstein S, Goetz JD, Rothstein A.  $\text{Na}^+$  fluxes in thymic lymphocytes. II. Amiloride-sensitive  $\text{Na}^+/\text{H}^+$  exchange pathway; reversibility of transport and asymmetry of the modifier site. *J Gen Physiol* **84**:585-600, 1984.
21. Erne P, Burgisser E, Buhler FR, Dubach B, Kuhn H, Meier M, Rogg H. Enhancement of calcium influx in human platelets by CGP 28392, a novel dihydropyridine. *Biochem Biophys Res Commun* **118**:842-847, 1984.
22. Resink TJ, Dimitrov D, Zschauer A, Erne P, Tkachuk VA, Buhler FR. Platelet calcium-linked abnormalities in essential hypertension. In: Bianchi G, Carafoli E, Scarpa A, Eds. *Membrane Pathology*. New York: New York Academy of Science, Vol **488**: pp252-265, 1986.
23. Cragoe EJ Jr, Woltersdorf OW Jr, Bicking JB, Kwong SF, Jones JH. Pyrazine diuretics. II. N-Amidino-3-amino-5-substituted-6-halopyrazinecarboxamides. *J Med Chem* **10**:66-75, 1967.
24. Thomas JA, Buchsbaum RN, Zimniak A, Racker E. Intracellular pH measurements in Ehrlich ascites tumor cells utilizing spectroscopic probes generated *in situ*. *Biochemistry* **18**:2210-2218, 1979.
25. SAS Introductory Guide for Personal Computers. SAS Institute Inc., Cary, NC, 1988.
26. Semplicini A, Spalvins A, Canessa M. Kinetics and stoichiometry of the human red cell  $\text{Na}^+/\text{H}^+$  exchanger. *J Memb Biol* **107**:219-228, 1989.
27. Otsu K, Kinsella J, Saktor B, Froehlich JP. Transient state kinetic evidence for an oligomer in the mechanism of  $\text{Na}^+/\text{H}^+$  exchange. *Proc Natl Acad Sci USA* **86**:4818-4822, 1989.
28. Hopp L, Nakamura A, Kino M, Kuriyama S, Aviv A. Refined evaluation of the exponential curve parameters and initial exchange rate constant for  $^{22}\text{Na}^+$  washout in cultured human skin fibroblasts. *Proc Soc Exp Biol Med* **188**:70-76, 1988.